

PHOTOLUMINESCENCE CHARACTERIZATION OF Te-DOPED GaSb FOR TPV APPLICATIONS

A.S. Vlasov, V.P. Khvostikov, E.P. Rakova, S.V. Sorokina, and V.M. Andreev
A.F. Ioffe Physical-Technical Institute
26 Polytechnicheskaya, St. Petersburg, Russia, 194021

ABSTRACT: Photoluminescence characterization of Czochralski-grown Te-doped GaSb wafers is presented. The wafers with the doping level from $2 \cdot 10^{17} \text{ cm}^{-3}$ to $2 \cdot 10^{18} \text{ cm}^{-3}$ have been studied. Calculations of photoluminescence line shape of Te-doped GaSb wafers at 77 K have been performed. It is demonstrated that the photoluminescence line shape analysis can be used for the native defect concentration estimation. The doping level obtained from the photoluminescence data is correlated with the results of the Hall mobility measurements. The native defect concentration has been obtained with the help of the developed analysis. A comparative study of photovoltaic cells manufactured from different wafers is presented. It is shown that the defect concentration obtained by the photoluminescence measurements can be treated as a reference value for material characterization.

Keywords: GaSb, photoluminescence, Czochralski, defects

1 INTRODUCTION

GaSb is the most promising material for TPV applications, for a good performance and a cheap and easy diffusion technology used for the TPV cell manufacture. GaSb is known to have a very high native defects concentration, which depends on the various growth conditions [1]. The origin of these defects is controversial. Based on the assumption of Van der Muellen [2] (who investigated the diffusion coefficients of these recombination centers), the p-type natural conductivity of GaSb was attributed to the high $V_{\text{Ga}}G_{\text{Sb}}$ complex defects concentration, which act as doubly ionizable native acceptors (N_A).

Experimental investigations of Rühle [3] indicated simpler (non-complex) native defects structure. Thermodynamical [4] and first-principles [5] calculations suggest that the most probable defect is Ga_{Sb} antisite, which is also doubly ionizable. This result is in agreement with the recent profound study of Zn and Ga diffusion under Ga-rich conditions performed by Bracht et al. [6], showing the experimental evidences of antisite Ga_{Sb} defect dominance in GaSb. Nevertheless, the origin of these defects is, their concentration is high. The hole concentration at 300 K of the undoped material ranges from 10^{16} cm^{-3} for MBE [7] or MOCVD [8] grown material to $2 \cdot 10^{17}$ and higher for the Czochralski grown bulk wafers [9]. Presumably, this concentration is ruled by native defects. This difference occurs, most probably, from the growth conditions, which are Sb-rich for the MBE or MOCVD processes and Ga-rich for Czochralski process. It should be noted, that the properties of the Czochralski grown ingots are normally non-uniform, even the properties of the substrates cut from different ingot parts may scatter significantly [10]. Therefore, an effective method for the material characterization is required for choosing a proper ingot part for the device fabrication. The most widespread means for the material characterization is the Hall mobility measurement. According to the calculations presented in [11] the mobility depends on the native defect concentration.

2 THEORETICAL APPROACH

Photoluminescence of GaSb has been studied

intensively [1] during the past two (or even four) decades. However, the quality of the investigated material and its properties due to various dopants and technology differs. The results of PL lineshape calculations, made in accordance with the method elaborated in the manuscript [12] with some specific changes introduced to account for the high native acceptor concentration of Czochralski grown GaSb wafers. The aim of the present study was to apply the photoluminescence lineshape analysis to the estimation of the native defect concentration and to find a correlation between the PL lineshape and photovoltaic cell properties.

The photoluminescence lineshape is given by an integral, which accounts for the electrons' and holes' energies, densities of states (DOS) and occupation probabilities.

For the description of the band tailing due to the high doping concentration, two models have been applied: a semiclassical Kane theory [13] of the band tailing and an interacting Fermi liquid model [14]. The second model introduces a more pronounced band tailing effect. It appeared, that, even at high doping concentrations (up to $n \sim 2 \cdot 10^{18} \text{ cm}^{-3}$), the Kane theory gives better fit to the experimental spectra. The most heavily doped samples seem to exhibit slightly more pronounced band tails than the Kane model predictions. Band gap narrowing due to the Hartree-Fock exchange interaction was introduced as well.

3 RESULTS AND DISCUSSION

The Te-doped GaSb wafers were received from different manufactures: Girmet Ltd., Electronics and Information Technology Laboratory of the French Atomic Energy Commission (LETI-CEA) and Wafer Technology Ltd. The doping level varied from $2 \cdot 10^{17} \text{ cm}^{-3}$ to $2 \cdot 10^{18} \text{ cm}^{-3}$.

The PL spectra measurements were performed at liquid nitrogen temperature with the MDR-23 spectrometer in the wavelength region of 1450 - 2000 nm with resolution of $\sim 2.4 \text{ nm}$. The photoluminescence was excited by CW 532 nm ND: YAG-laser, the pumping power density varied from 1 to 500 W/cm^2 .

Analysis of the experimental PL spectra was performed in the following manner. First, the initial

doping concentration is chosen in concordance with the PL peak position. The native defect concentration is set to $2 \times 10^{17} \text{ cm}^{-3}$ and the spectra are fitted, so that the only changeable parameter is the hole quasi-Fermi level position. Next, the doping level is changed slightly, and the fitting is repeated. Thereby, a native defect concentration value is obtained at each step. When the minimal native defect concentration is found, the iteration is completed.

There's some systematic difference in the NA values obtained by PL and Hall data analysis, which may result from the different approaches to the defect concentration. In the case of the Hall data, the singly or doubly (in the brackets) ionized acceptors concentration values are indicated. In the case of PL measurements, two types of the acceptors (complex Te born ones and native) are contributing to the PL spectra in the samples with the doping level below $7\text{-}8 \times 10^{17} \text{ cm}^{-3}$. Estimation of each acceptor concentration exact value is possible only by introducing the carrier capture and recombination rate of each center, which will introduce additional parameters to the calculation and complicate it. The data available for GaSb is insufficient for such an estimation, thus the defect concentration obtained by the PL measurements (as well as the estimation from the Hall mobility) may be treated only as a reference value, that controls the DOS tails and acceptor level broadening and can be used for the samples comparing.

Figure 1 presents an example of the fitting results at different excitation densities. A good quality the fitting procedure can be seen from this figure. The main band consists of two parts known as C (an ionized state of the native acceptor, activation energy $\sim 105 \text{ meV}$) and T (tellurium and native acceptor complex, activation energy $\sim 72 \text{ meV}$) bands. Also, a weak line can be detected at 0.65 eV (which corresponds to approx. $\sim 150 \text{ meV}$ level position). The intensity of this line is proportional to the intensity of the C-line component, and it disappears completely in a heavily doped sample, what indicates that this line is bound to the native acceptor state.

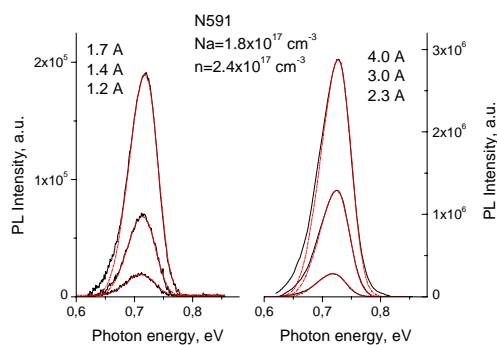


Fig. 1. PL spectra of N591 sample ($n_{\text{Hall}} = 2.5 \times 10^{17} \text{ cm}^{-3}$) measured at different excitation power. Solid lines experimental, dashed lines calculated ones with parameters $n = 2.4 \times 10^{17} \text{ cm}^{-3}$, $N_A = 1.8 \times 10^{17} \text{ cm}^{-3}$.

Table 1 presents the results of the PL spectra fitting in comparison with the independent Hall hole mobility measurements. The values of the native defect concentration are an estimation based on the Baxter et al. calculations [11].

Table I. Results of the PL lineshape analysis in comparison with the Hall data.

Sample	n(Hall), cm^{-3}	n(PL), cm^{-3}	NA(PL), cm^{-3}	NA(Hall), cm^{-3}
N591	2.5 $\times 10^{17}$	2.4 $\times 10^{17}$	1.8 $\times 10^{17}$	2.6 (0.85) $\times 10^{17}$
RG5	2.4 $\times 10^{17}$	2.4 $\times 10^{17}$	2.1 $\times 10^{17}$	3.5 (1.2) $\times 10^{17}$
N178	5.5 $\times 10^{17}$	5.0 $\times 10^{17}$	2.3 $\times 10^{17}$	3.0 (1.0) $\times 10^{17}$

The described GaSb wafers were used for PV cell fabrication by a double stage Zn diffusion technology. The details of the technology are described elsewhere [15]. A comparative study of the cells obtained on different wafers is presented below. Figure 2 presents the internal quantum yield of three samples N591 (solid line), RG5 (dash-dotted line) and N178 (dotted line), (see Table I for N_A value). The low energy part of the spectral photoresponse, which is responsible for the diffusion length in the diodes with a relatively short emitter, is shown. It can be seen that the RG5 and N178 samples reveal lower performance than N591 one.

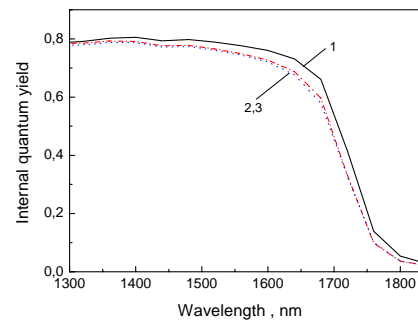


Fig. 2. Long wavelength parts of the spectral photoresponse curves. PV cells are made of the following materials: solid line N591 ($N_A = 1.8 \times 10^{17} \text{ cm}^{-3}$), dashed line RG5 ($N_A = 2.1 \times 10^{17} \text{ cm}^{-3}$), dash-dotted line N178 ($N_A = 2.3 \times 10^{17} \text{ cm}^{-3}$).

Figure 3 presents resistanceless dark J-V_J curves of three PV cells (3.5x3.5 mm) made of RG5, N178 and N591 ingots. The method used for resistanceless diode characterization is described in [16]. The recombination-related (J_0^{rek}) and diffusion-related (J_0^{diff}) components obtained from these measurements are listed in Table II. It can be seen that the recombination-related part of the I-V characteristic, which is responsible for the carrier recombination through the localized states in the p-n junction, is in strict accordance with the native defect concentration values obtained from the photoluminescence characterization.

There's a considerable difference between the N178 and RG5 samples in the diffusion-related component, which may originate from different growth conditions used by different substrate manufacturers. The population density of various defects depends on the growth conditions: e.g. reduction of GaSb concentration is accompanied by an increase in Sb_{Ga} or V_{Ga} defect concentration. In turn, the diffusion process is based on

different mechanisms involving point defects [6], and a great difference in diffusion-related component may result from a different Zn diffusion profile (lower p-n junction thickness), resulting from a different point defect content. This, however, is not the question of the present study.

Table II: Current flow components obtained from the resistanceless $J-V_j$ measurements.

Sample	J_0^{rek} , $\times 10^{-5} \text{ A/cm}^2$	J_0^{diff} , $\times 10^{-9} \text{ A/cm}^2$	NA^{PL} , $\times 10^{17} \text{ cm}^{-3}$
N178	8	4.9	2.3
RG5	6	26	2.1
N591	4	1.9	1.8

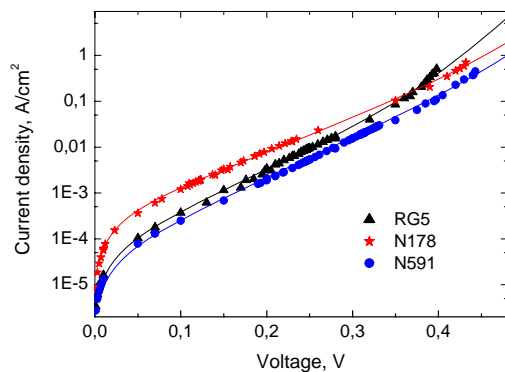


Fig. 3. Resistanceless dark $J-V_j$ characteristics of PV cells' $p-n$ junctions made of RG5 (triangles), N178 (stars) and N591 (circles) ingots. Solid lines are calculated curves, fitting to the experimental ones.

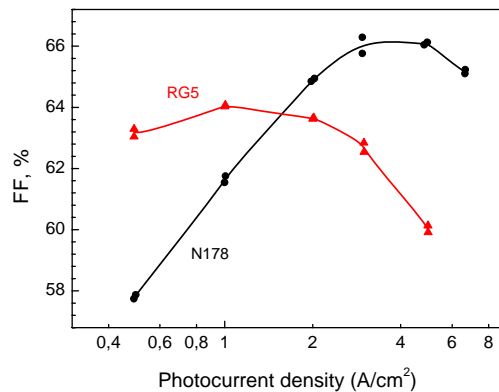


Fig. 4. Dependence of the Fill factor values of the structures made of the two studied wafers N178 (circles) and RG5 (triangles).

Figure 4 presents a fill factor (FF) vs photocurrent density dependence for two PV cell structures. It can be seen from the figure, that the results obtained with resistanceless I-V curve measurements are confirmed. At low current densities ($J_{\text{SC}} \leq 1 \text{ A/cm}^2$) FF values are controlled by the recombination-related component, and structures with lower native defect concentration reveal better performance, while at higher current densities the I-V curve shape is controlled by the diffusion-related term, which depends basically on the transport properties of the charge carriers and the p-n junction thickness (i.e.

the Zn diffusion profile). It should be noted here, that both structures reveal close values of the I-V curve derivative near the V_{OC} point (0.4-0.5 V), indicating that the discussed difference in the fill factor behavior is not connected with any shunt resistance.

4 SUMMARY

A quantitative method of the photoluminescence line shape analysis has been presented. It has been demonstrated that this method could be used for the characterization of the material properties i.e. the native defects concentration. The self-consistent results of the photoluminescence lineshape analysis are in a good agreement with the Hall measurement data. GaSb TPV cells have been manufactured and characterized. The cell photoresponse and I-V characteristics are found to be in strict correspondence with the PL analysis results.

5 ACKNOWLEDGEMENTS

Special thanks to N.Kh. Timoshina and M.Z. Swarts for PV cell photoresponse and I-V curve measurements and discussion of the results. This work was supported by RFBR grants No 09-08-00243 and 07-08-13526.

6 REFERENCES

- [1] P.S. Dutta, H.L. Bhat, and V. Kumar, *J. Appl. Phys.* 81 (9) pp. 5821-70 (1997)
- [2] Y.J. Van der Meulen, *J. Phys. Chem. Solids*, 28 pp. 25-32 (1967)
- [3] W. Ruhle and D. Bimberg, *Phys. Rev. B* 12 (6) pp. 2382-90 (1975)
- [4] M. Ichimura, K. Higuchi, Y. Hattori, and T. Wada, *J. Appl. Phys.* 68 (12) pp. 6153-58 (1990)
- [5] M. Hakala, M.J. Puska, and R.M. Nieminen, *J. Appl. Phys.* 91 (8) pp. 4988-94 (2002)
- [6] K. Sunder, H. Bracht, S. P. Nicols, and E.E. Haller, *Phys. Rev. B* 75 pp. 245210-1-9 (2007)
- [7] A.Y. Polyakov, M. Stam, A.G. Milnes, R.G. Wilson, Z.Q. Fang, P. Rai-Choudhury, and R.J. Hillard, *J. Appl. Phys.*, 72 (4) 1316 (1992)
- [8] R.V. Levin, A.S. Vlasov, N.V. Zotova, B.A. Matveev, B.V. Pushnyi, and V.M. Andreev, *Semiconductors*, 40 (12) 1393 (2006)
- [9] B. Stepanek, V. Sestakova, and J. Sestak, *Proc. of SPIE*, 4412 p.46 (2001)
- [10] V.P. Khvostikov, S.V. Sorokina, N.S. Potapovich, O.A. Khvostikova, A.S. Vlasov, E.P. Rakova, and V.M. Andreev, *Semiconductors* 42(10) 1179 (2008)
- [11] R.D. Baxter, F.J. Reid, and A.C. Beer, *Phys. Rev.* 162 (3) pp. 718-727 (1967)
- [12] A. Bignazzi, A. Bosacchi, and R. Magnanini, *J. Appl. Phys.* 81 (11) pp. 7540-47 (1997)
- [13] E.O. Kane, *Phys. Rev.* 131 (1) pp. 79-88 (1963)
- [14] P. Van Mieghem, *Rev. Mod. Phys.* 64 (3) pp. 755-93 (1992)
- [15] V.P. Khvostikov, M.G. Rastegaeva, O.A. Khvostikova, S.V. Sorokina, A.V. Malevskaya, M.Z. Shvarts, A.N. Andreev, D.V. Davydov and V.M. Andreev, *Semiconductors*, 40 (10) pp. 1275-1279 (2006)
- [16] V.M. Andreev, V.V. Evstropov, V.S. Kalinovsky, V.M. Lantratov, and V.P. Khvostikov, *Semiconductors*, 43 (5) pp. 644-651 (2009)